Connecting Atmospheric Blocking to European Temperature Extremes in Spring

LUKAS BRUNNER

Wegener Center for Climate and Global Change (WEGC), Institute for Geophysics, Astrophysics, and Meteorology/Institute of Physics, and Fonds zur Förderung der wissenschaftlichen Forschung—Doktoratskolleg (FWF-DK) Climate Change, University of Graz, Graz, Austria

GABRIELE C. HEGERL

School of Geosciences, University of Edinburgh, Edinburgh, United Kingdom

ANDREA K. STEINER

Wegener Center for Climate and Global Change (WEGC), Institute for Geophysics, Astrophysics, and Meteorology/Institute of Physics, and Fonds zur Förderung der wissenschaftlichen Forschung—Doktoratskolleg (FWF-DK) Climate Change, University of Graz, Graz, Austria

(Manuscript received 13 July 2016, in final form 28 October 2016)

ABSTRACT

Atmospheric blocking is an important contributor to European temperature variability. It can trigger cold and warm spells, which is of specific relevance in spring because vegetation is particularly vulnerable to extreme temperatures in the growing season. The spring season is investigated as a transition period from predominant connections of blocking with cold spells in winter to predominant connections of blocking with warm spells in summer. Extreme temperatures are termed cold or warm spells if temperature stays outside the 10th to 90th percentile range for at least six consecutive days. Cold and warm spells in Europe over 1979–2014 are analyzed in observations from the European daily high-resolution gridded dataset (E-OBS) and the connection to blocking is examined in geopotential height fields from ERA-Interim. A highly significant link between blocking and cold and warm spells is found that changes during spring. Blocking over the northeastern Atlantic and Scandinavia is correlated with the occurrence of cold spells in Europe, particularly early in spring, whereas blocking over central Europe is associated with warmer conditions, particularly from March onward. The location of the block also impacts the spatial distribution of temperature extremes. More than 80% of cold spells in southeastern Europe occur during blocking whereas warm spells are correlated with blocking mainly in northern Europe. Over the analysis period, substantial interannual variability is found but also a decrease in cold spells and an increase in warm spells. The long-term change to a warmer climate holds the potential for even higher vulnerability to spring cold extremes.

1. Introduction

European weather and climate are strongly influenced by large-scale circulation patterns such as the Atlantic storm tracks, the jet stream, and atmospheric blocking (e.g., Woollings 2010). Atmospheric blocking describes a meteorological situation in which a persistent and stationary high pressure system blocks the climatological westerly flow at midlatitudes for several days to weeks (Rex 1950; Tibaldi and Molteni 1990; Pelly and Hoskins 2003; Barriopedro et al. 2006; Croci-Maspoli et al. 2007).

Extremes on both ends of the temperature distribution are especially closely connected to atmospheric blocking. Increased cold spell frequency is found during blocked conditions in European winter (Buehler et al. 2011) and up to 80% of summer hot temperature extremes in northern Europe are associated with a collocated blocking (Pfahl and Wernli 2012). Atmospheric blocking has also been identified as main contributor to specific extreme events such as the cold European winter in 2010 (Cattiaux et al. 2010) and the Russian heatwave in summer 2010 (Matsueda 2011).

Surface temperatures can be impacted by atmospheric blocking via radiative forcing or advection. Radiative

Denotes Open Access content.

Corresponding author e-mail: lukas.brunner@uni-graz.at

DOI: 10.1175/JCLI-D-16-0518.1

effects are mainly constrained to the center of the block where clear-sky conditions favor positive temperature anomalies. The anticyclonic circulation of the block affects temperatures especially on the eastern and southern flanks by advection of cold air from the north and east (e.g., Trigo et al. 2004; Bieli et al. 2015). A range of studies have focused on either the predominant cooling effect of blocking in winter (Trigo et al. 2004; Barriopedro et al. 2008; Cattiaux et al. 2010; Buehler et al. 2011; Sillmann et al. 2011; Whan et al. 2016) or the warming effect in summer (Xoplaki et al. 2003; Cassou et al. 2005; Pfahl and Wernli 2012; Stefanon et al. 2012). Recently, Cassou and Cattiaux (2016) showed that the transition from blocking being linked to anomalously cold conditions in winter to blocking being linked to warm conditions in summer has shifted by a few days because of climate warming.

Here we investigate the link between atmospheric blocking and European cold and warm spells during spring to provide better insight into the shifting role of blocking for extremes during this transition period. Spring temperature extremes are of special relevance because vegetation during this season is particularly vulnerable to abnormal temperatures. Late spring frost can severely harm or even destroy fresh leaves, subsequently requiring considerable additional resource use by plants. Correspondingly, warm spells in early spring can lead to premature greening onset (Hufkens et al. 2012; Menzel et al. 2015, and references therein). Ma et al. (2016) showed the potential of earlier spring green-up to also impact European warm spells via feedback processes. In this study we analyze the connection of blocking and extreme temperature occurrences, noting their spatial distribution and change over the last decades. We focus on spring on a month-by-month basis but also show results for the seasonal mean of other seasons. We describe data and methods in section 2. Results are presented in section 3 and a summary is given in section 4.

2. Data and methods

The detection of temperature extremes is based on the European daily high-resolution gridded dataset (E-OBS), version 12.0 (Haylock et al. 2008), an observational land-only dataset for Europe. It comprises measurements from a network of more than 2000 irregularly distributed meteorological stations interpolated to a regular grid (Klok and Klein Tank 2009). In this study we investigate daily minimum temperature $T_{\min}$ and daily maximum temperature $T_{\max}$ on a 0.25° × 0.25° longitude–latitude grid between 1979 and 2014. We detect cold and warm spells over mainland Europe and the British Isles (35°–72.5°N, 12.5°W–30°E). First, the daily linear trend from 1979 to 2014 is subtracted from each grid point in the E-OBS temperatures to remove the long-term temperature trend. Daily 10th and 90th percentiles of $T_{\min}$ and $T_{\max}$ are computed, respectively, over the 36-yr period using a 21-day sliding window. A grid point with $T_{\min}$ below the 10th percentile or $T_{\max}$ above the 90th percentile for at least six consecutive days is identified as a cold or warm extreme, respectively. This study focuses on large-scale events on a daily basis. Therefore we define a cold spell day (CSD) or warm spell day (WSD) if at least 400 grid points (i.e., a 5° × 5° region) simultaneously are found to be exposed to a cold or warm extreme criterion on a given day. Resulting cold and warm spells are found to be spatially highly coherent, so no separate adjacency criterion was applied.

The detection of blocking is based on daily geopotential height (GPH) fields from ERA-Interim (Dee et al. 2011) at a 2.5° × 2.5° longitude–latitude grid, which is available from 1979 onward. We apply a standard algorithm utilizing the reversal of midlatitude 500-hPa GPH gradients (Tibaldi and Molteni 1990; Scherrer et al. 2006; Davini et al. 2012, 2014), detailed in Brunner et al. (2016). The blocking detection algorithm identifies high pressure systems associated with an overturning of the flow and selects extended and persistent events of at least five days duration. Therefore this classical approach covers stationary and isolated high pressure systems northward of 45°N. We compute blocking frequencies on a grid point basis for climatological conditions as well as for CSDs and WSDs. We subsequently define a blocked day if blocking is found anywhere in the Euro-Atlantic blocking region (45°–72.5°N, 30°W–45°E) (Barriopedro et al. 2010; IPCC 2013) on a certain day. We then also investigate the relative frequency of CSDs and WSDs on a grid point basis during blocked and unblocked days. This approach allows us to simultaneously investigate the local and remote effects of blocking on CSDs and WSDs.

In addition, we analyze selected subdomains and investigate the importance of the location of cold and warm spells and blocking for their connection. For selection of CSDs and WSDs in subdomains we adjust the spatial criterion to consider CSDs and WSDs with more than half of their grid points in the selected subdomain. For selection of blocking in subdomains we consider blocks with at least one blocked grid point in the selected subdomain.

To test any co-occurrence of CSDs and WSDs and blocked days for significance we perform a Monte Carlo test. Given N CSDs or WSDs in a period (i.e., month or season), we draw 1000 random samples of N days from the same period. To ensure that each random sample yields the same autocorrelation at all lags the samples

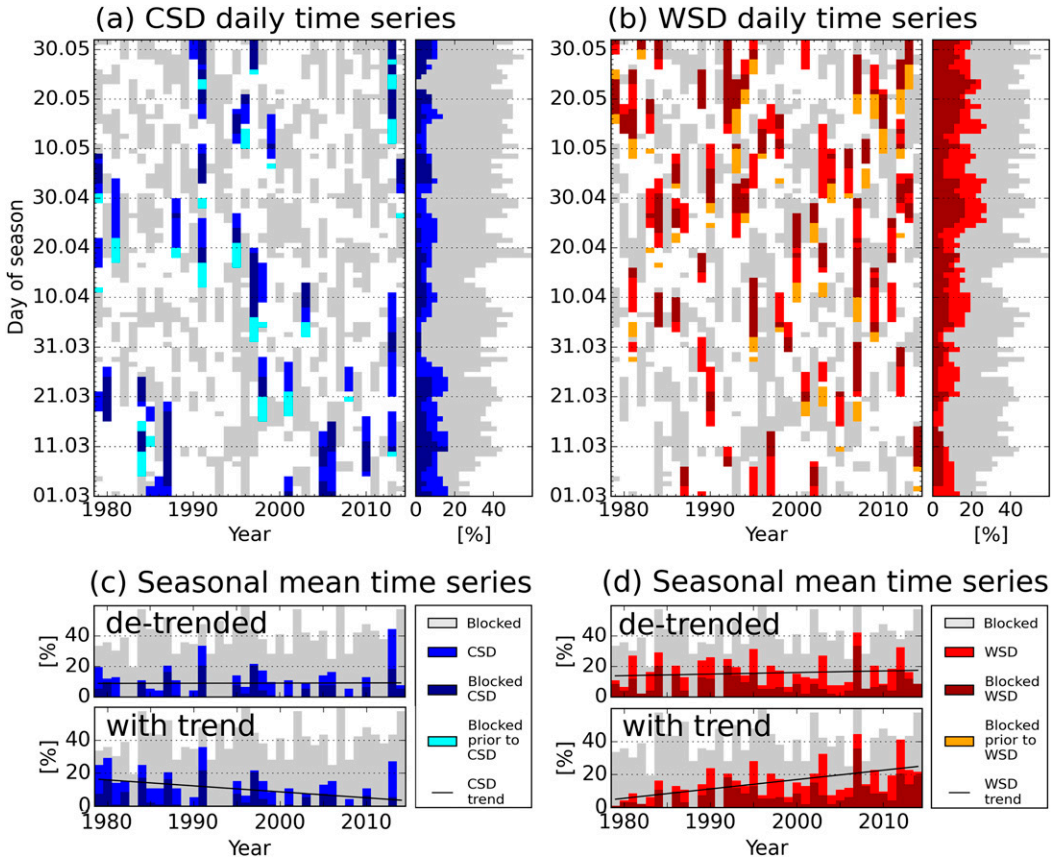

FIG. 1. Time evolution of blocking for (a) CSDs and (b) WSDs in European spring based on detrended data. The left panels in (a),(b) show blocked days in gray, cold (warm) spell days in blue (red), blocked cold (warm) spell days in dark blue (dark red), and blocking within 5 days before a cold (warm) spell day in turquoise (orange). The right panels in (a),(b) show percentages for each day during spring based on 36 years from 1979 to 2014. The seasonal mean time series are shown for (c) CSDs and (d) WSDs where the trend was removed (top plots) and not removed (bottom plots) from the underlying temperature time series.

are drawn as clusters of days similar as represented in the original dataset. We then calculate for each random sample of N days the blocking frequency on a grid point basis as well as the occurrence of blocked days in the blocking region. The correlation between blocking and CSDs or WSDs is considered statistically significant if the blocking frequency during CSDs and WSDs on a grid point or if the number of blocked CSDs or WSDs is smaller than the 5th percentile or larger than the 95th percentile of the joined probability density function (PDF) established over all 1000 random samples, respectively. The same considerations are made for the statistical significance of CSDs and WSDs given the number of blocked days in each period.

3. Results

The time evolution of blocked and extreme days is presented in Fig. 1. Over the spring season (MAM), a decrease in the number of CSDs (both generally and also if restricted to blocked days) is found toward late spring (Fig. 1a, right). Over 1979–2014, the seasonal mean time series (Fig. 1c, top) shows periods with less or more CSDs, pointing at significant interannual variability. A considerable number of CSDs exhibit blocking several days before their onset, indicating that a certain amount of time is necessary to lower the temperature sufficiently for a cold spell to develop (Fig. 1a, left), consistent with findings of Buehler et al. (2011). If the trend in the underlying temperature time series is not removed (Fig. 1c, bottom) we find more CSDs at the beginning of the period and a lack of CSDs at the end of the period, indicating that extended cold periods are constrained to winter in a warming climate. However, some lack of cold spells also occurs after detrending (Fig. 1c, top), pointing at the role of internal variability.

Over the spring season, the number of WSDs and with it the number of blocked WSDs increases toward

TABLE 1. Overview on statistics of CSDs, WSDs, and blocked days. Columns from left to right: Period name and number of total days per (top) season and (bottom) month, number of blocked days (percentage of total days), number of CSDs (percentage of total days), number of WSDs (percentage of total days), number of blocked CSDs (percentage of blocked days/percentage of CSDs), and number of blocked WSDs (percentage of blocked days/percentage of WSDs). Entries with the number of blocked CSDs and WSDs above (below) the 95th (5th) percentile are indicated in boldface (italics).

Period	Days	Blocked days	CSDs	WSDs	Blocked CSDs	Blocked WSDs
MAM	3312	1363 (41.15%)	299 (9.03%)	519 (15.67%)	139 (10.20%/46.49%)	**280 (20.54%/53.95%)**
JJA	3312	961 (29.02%)	81 (2.45%)	565 (17.06%)	*11* (*1.14%*/*13.58%*)	**301 (31.32%/53.27%)**
SON	3276	1025 (31.29%)	308 (9.40%)	421 (12.85%)	116 (11.32%/37.66%)	138 (13.46%/32.78%)
DJF	3240	1176 (36.30%)	554 (17.10%)	361 (11.14%)	**297 (25.26%/53.61%)**	*102* (*8.67%*/*28.25%*)
Feb	1008	423 (41.96%)	157 (15.58%)	103 (10.22%)	**93 (21.99%/59.24%)**	*24* (*5.67%*/*23.30%*)
Mar	1116	395 (35.39%)	135 (12.10%)	105 (9.41%)	61 (15.44%/45.19%)	46 (11.65%/43.81%)
Apr	1080	449 (41.57%)	80 (7.41%)	183 (16.94%)	27 (6.01%/33.75%)	**99 (22.05%/54.10%)**
May	1116	519 (46.51%)	84 (7.53%)	231 (20.70%)	51 (9.83%/60.71%)	**135 (26.01%/58.44%)**
Jun	1080	393 (36.39%)	30 (2.78%)	181 (16.76%)	*4* (*1.02%*/*13.33%*)	**111 (28.24%/61.33%)**

summer (Fig. 1b, right). Over the analysis period, the seasonal mean time series also show considerable interannual variability for WSDs (Fig. 1d, top). If the trend is not removed from the underlying temperature time series (Fig. 1d, bottom) an increase of the number of WSDs (both, generally and if restricted to blocked conditions) in the investigated period from 1979 to 2014 is evident, consistent with the detection of changes in the number of temperature extremes in Europe (Zwiers et al. 2011; IPCC 2013; Morak et al. 2013). Note that all subsequent discussions refer exclusively to the detrended data.

A complete summary of statistics for CSDs and WSDs in spring and all individual months of the extended spring season (February–June) is shown in Table 1. We also included results for the summer (JJA), fall (SON), and winter (DJF) seasons for comparison. Our results generally indicate that blocking plays a strong role in spring–summer warm spells and in fall–winter cold spells, consistent with the literature (e.g., Cassou and Cattiaux 2016). In total about 46% of CSDs in spring are blocked days and about 10% of blocked spring days coincide with a CSD. A statistically significant link is found in the extended spring season in February (correlation) and June (anticorrelation) as well as in winter (correlation) and in summer (anticorrelation; cf. Table 1). Regarding WSDs in spring, a statistically significant fraction of 54% is blocked and about 21% blocked spring days coincide with a WSD. Also, most individual months of the extended spring show a significant correlation with blocking (as do summer months); however, February on the transition from winter to spring exhibits a significant anticorrelation (as do winter months; cf. Table 1).

Analyzing blocking on a grid point basis, the climatological blocking frequency in the Euro-Atlantic region is generally between 2% and 6% of spring days. The blocking frequency coinciding with CSDs in spring is depicted in Fig. 2a. Three distinct regions are revealed: west of the British Isles (region 1) and over northern Scandinavia (region 2) the blocking frequency is up to 3 times higher for CSDs than for climatological conditions and differs statistically significantly from the random sample. This is consistent with cold advection during such blocks into central and western Europe. Over central and eastern Europe (region 3) there is significantly less blocking during CSDs (<2%) than in the climatology since blocking occurring there tends to lead to warmer, fair-weather conditions.

A closer investigation of the extended spring season based on monthly frequencies reveals how the role of blocking associated with CSDs changes through spring (Figs. 2b–f). February and March show significantly increased blocking frequency northward of 60°N (exceeding 16% and 12%, respectively), indicating a strong link of blocking in this region to cold conditions in Europe in late winter–early spring. Between March and April a distinct change is obvious such that maximum blocking frequencies shift from northern Europe to the west of the British Isles. This change may be founded in the temperature seasonality over the European continent: in winter the continent is still relatively cold, such that easterly flow is sufficient to lead to CSDs, while northerly advection with blocking to the west is necessary as the continent warms up in later spring. The CSD blocking frequency in central and eastern Europe is lowered during all spring months, highlighting the anticorrelation between cold conditions and blocking in this region. In June where only about 3% of total days are associated with a cold spell (cf. Table 1) no significant relationship with blocking is found.

The blocking frequency coinciding with WSDs in spring is found to be up to 3 times higher than during climatological conditions (Fig. 3a) and statistically

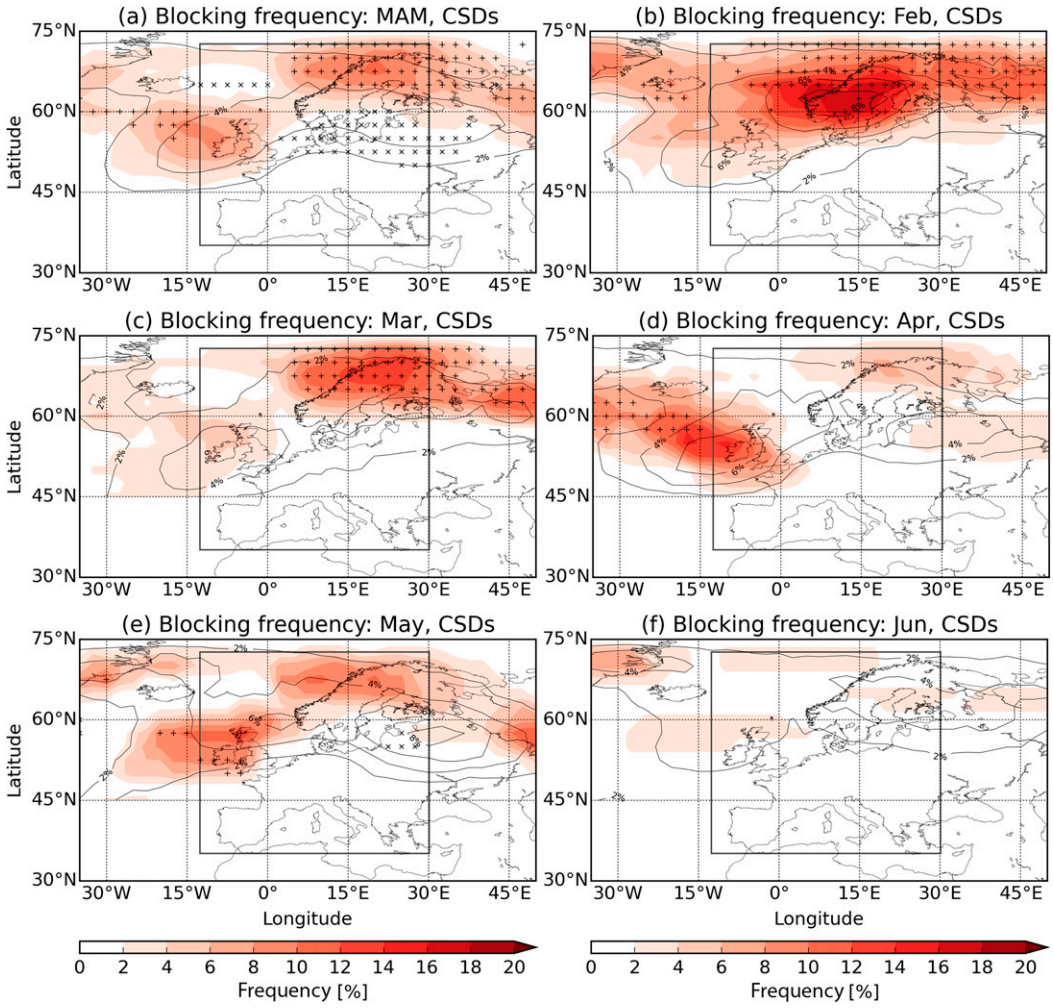

FIG. 2. Blocking frequency per grid point (shading) coinciding with CSDs in the European region (gray box) for (a) spring (MAM), (b) February, (c) March, (d) April, (e) May, and (f) June. Values that are statistically significantly larger than the number of blocks from random days (above 95th percentile) are marked with a plus sign and values that are statistically significantly lower (below 5th percentile) are marked with a multiplication sign. The climatological blocking frequency is indicated by black contour lines.

significantly different from the random sample in most of Europe. Blocks linked to warm spells are distributed across Europe, whereas there are fewer than average blocking days associated with WSDs west of the British Isles. The anticyclonic motion of blocking highs in the latter area would favor cold advection into Europe, consistent with the results for CSDs (Fig. 2).

Resolving individual months (Figs. 3b–f) reveals that in February the link between blocking and WSDs is mostly negative. Over the entire winter season, a significant and widespread anticorrelation is found between warm spells and blocking in the west and north of the Euro-Atlantic blocking region (not shown). However, over central Europe increased blocking frequencies on WSDs can be found in February and in winter, indicating that fair-weather conditions connected with blocking highs can lead to winter warm spells here. From March onward the WSD blocking frequency shows a strong increase and is significantly higher than the climatological mean. The maximum of the frequency shifts slightly to the north toward summer.

Having analyzed the distribution of blocking frequencies, we now reversely investigate the spatial distribution of grid points contributing to CSDs and WSDs (termed CSDs and WSDs per grid point) in the European region. Figures 4a and 4b show the number of CSDs and WSDs per grid point over 36 springs from 1979 to 2014, respectively. The fraction of CSDs and WSDs per grid point during 1363 blocked days in spring

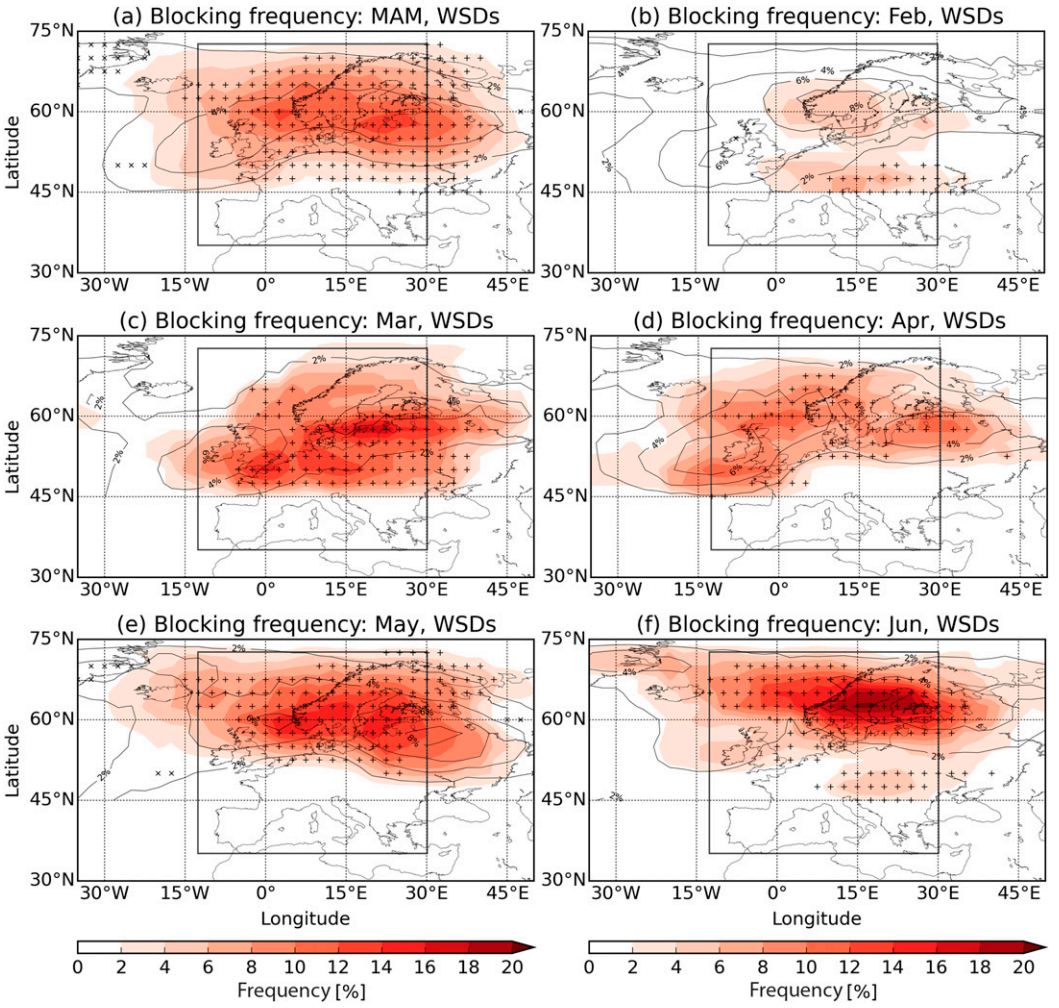

FIG. 3. As in Fig. 2, but for blocking frequency per grid point coinciding with WSDs.

(Figs. 4c,d) reveals a distinct dipole pattern for both cases. While in total about 46% of CSDs are blocked in spring (cf. Table 1), in southeastern Europe more than 80% of CSDs per grid point are blocked. In contrast, a strong anticorrelation is found over the British Isles and in Scandinavia, where less than 30% of CSDs per grid point coincide with blocking. For WSDs per grid point the opposite picture arises with locally more than 80% associated with blocking northward of 50°N. In southeastern Europe statistically significant anticorrelation is found with less than 40% of WSDs per grid point connected to blocking. This is consistent with the preferential location of blocks during WSDs, which is largely limited to northern Europe (Fig. 3), particularly later in spring. Differences for T_{min} and T_{max} composites of blocked minus unblocked CSDs and WSDs show a similar dipole pattern: both CSDs and WSDs with a blocking anywhere in the blocking region are warmer in Scandinavia and colder in mainland Europe than without a blocking.

For a closer investigation of the dipole feature we divide Europe into two subdomains for CSDs and WSDs: northern (>50°N) and southern (<50°N) Europe (cf. Figs. 4c,d). Selecting only CSDs and WSDs in these subdomains we show the corresponding blocking frequency in Fig. 5. For the 163 CSDs in northern Europe hardly any blocking is found in the entire Euro-Atlantic blocking region (Fig. 5a), indicating that blocking tends to counteract CSDs here. CSDs (136 days) in southern Europe (Fig. 5c) are clearly linked to the blocking regions west of the British Isles and over Scandinavia indicated by distinct maximum blocking frequencies exceeding 18%. Considering conversely only blocking west of the British Isles (cf. Fig. 2a), we consistently find correlation predominantly with CSDs in southeastern Europe. Considering only

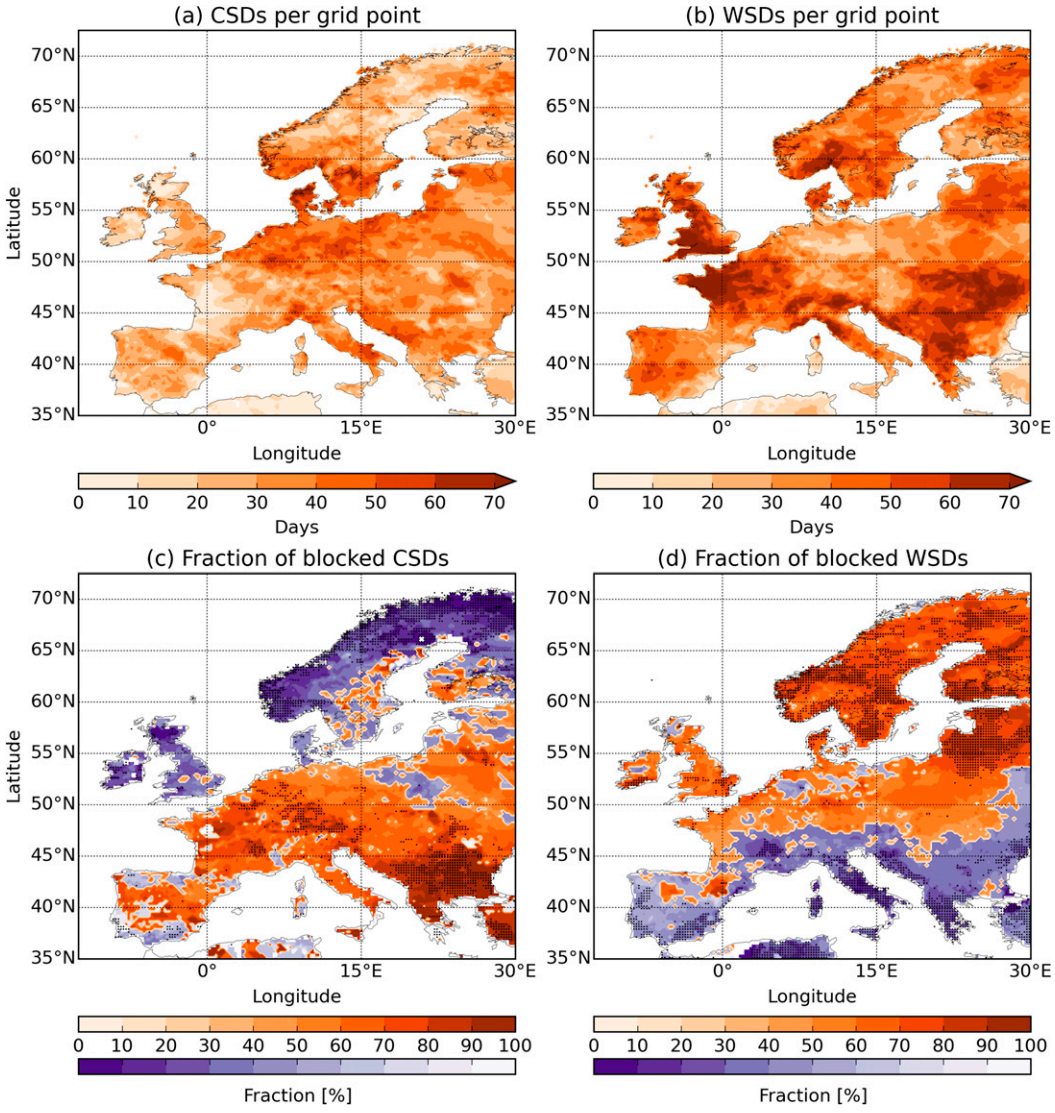

FIG. 4. Number of (a) CSDs and (b) WSDs per grid point in the European region over 36 springs from 1979 to 2014. Fraction of (c) CSDs and (d) WSDs per grid point during blocked days. Grid points where the fraction is above (below) the mean value of randomly drawn days are shown in orange (blue) shading. Grid points where the fraction is statistically significantly higher (above 95th percentile) or lower (below 5th percentile) than the random sample are marked with a dot.

blocking in northern Scandinavia (cf. Fig. 2a) leads to statistically significantly increased CSDs per grid point in most of central and eastern Europe (not shown).

WSDs in northern Europe (247 days) are found to be clearly connected to blocking over Scandinavia, with highest blocking frequencies exceeding 20% (Fig. 5b). Consistently, blocking over Scandinavia is correlated with increased frequency of WSDs in most of northern Europe in spring. In contrast, WSDs in southern Europe are connected to reduced blocking frequencies northward of 60°N (Fig. 5d). These results show the importance of the location of blocking and are consistent with a strong role of cold advection at the edges of blocks for CSDs and increased solar radiation leading to WSDs in blocked regions.

4. Summary and discussion

We analyzed the relationship between blocking occurrence and temperature extremes in European spring for the period 1979–2014. Our results show statistically significant correlations of blocking frequency and the occurrence of cold spells and warm spells throughout the spring season, with sensitivity to the location of the

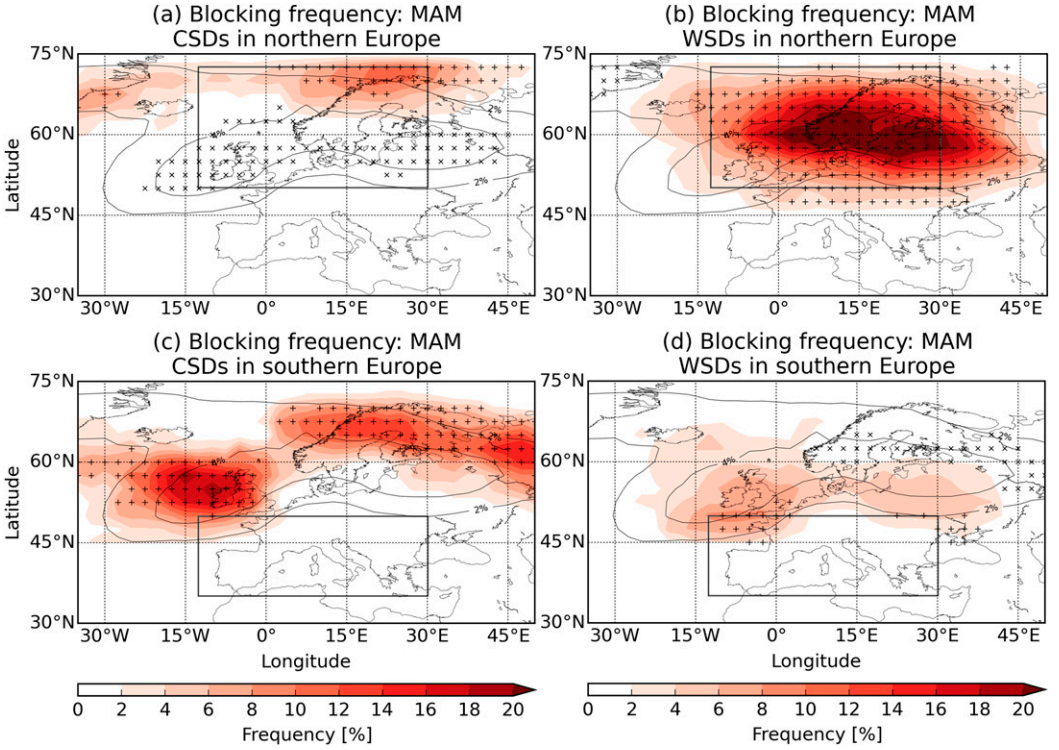

FIG. 5. Blocking frequency per grid point (shading) coinciding with (a),(c) CSDs and (b),(d) WSDs that occur over (top) northern and (bottom) southern Europe. The north–south split is at 50°N as indicated by the gray boxes. Values that are statistically significantly larger than the number of blocks from random days (above 95th percentile) are marked with a plus sign and values that are statistically significantly lower (below 5th percentile) are marked with a multiplication sign. The climatological blocking frequency is indicated by black contour lines.

block. We found blocking in winter and early spring to be stronger connected to cold conditions whereas blocking in late spring and summer is stronger connected to warm conditions. Blocked days in February show a statistically significant correlation with cold spell days whereas blocking in April is statistically significantly correlated to warm spell days, suggesting that on average the blocking–temperature relationship changes sign during this time.

Over the spring season, the number of cold spell days decreases toward late spring whereas the number of warm spell days increases. Over the analysis period, the seasonal mean time series shows considerable interannual variability for both cold and warm spells. If the trend is not removed from the underlying temperature time series, a lack of cold spell days and a clustering of warm spell days in late spring in the last 15 years of the investigated period suggest that the underlying long-term global warming trend also influences the frequency of cold spell days and warm spell days. In contrast, there is no apparent trend in the number of blocked days, suggesting that the trend is due to large-scale warming rather than a change in circulation. The shift in probability of less cold extremes toward a higher probability of warm extremes, particularly in late spring, is consistent with recent findings on the earlier onset of summer and disruption of the European seasonal clock (Cassou and Cattiaux 2016). In such a warmer climate the occurrence of a cold spell in spring becomes even more critical and detrimental to vegetation, as just recently happened in Europe. After exceptionally warm spring temperatures, central and southeastern Europe were affected by a cold spell in late April 2016 that caused great damage to crops, orchards, and vineyards, especially in Austria, Slovenia, Slovakia, and Croatia (AGRI4CAST 2016). Our findings lay the basis for further research into these changes, including the atmospheric dynamics driving the relationship of blocking and temperature extremes and potential contributions to improved seasonal forecasting.

The location of the block is also found to be essential for its impact on European extreme temperatures. Blocking west of the British Isles and over northern Scandinavia is clearly connected with cold spells in southern Europe whereas blocking over central Europe and southern Scandinavia is associated with warm spells

in northern Europe. This is consistent with the role of cold advection at the edges of blocks leading to cold spells outside blocked regions and with increased solar radiation leading to warm spells in blocked regions.

The spatial distribution of cold and warm spells during blocking reveals a distinct dipole pattern. Cold spells in southeastern Europe are found to be highly correlated with blocking, and more than 80% of cold spell days co-occur with a blocking. In contrast, cold spells in northern Scandinavia and blocking are anticorrelated with regionally less than 30% co-occurrence. Warm spells show the opposite relationship with locally more than 80% of warm spell days in northern Europe co-occurring with blocking, but anticorrelation in southern Europe. An increased occurrence of both warm and cold spells during blocked conditions is found around 50°N, indicating that blocking increases the probability for both high and low temperature extremes here.

The occurrence of atmospheric blocking in the European region is found to be crucial for the development of both extended cold and warm spells in spring. We provide insight into the changing role of blocking in spring as its connection to cold conditions decreases and the connection to warm conditions increases. Our findings furthermore underline the importance of the location of blocking for its correlation with either cold or warm spells, highlighting in particular the remote effects of blocking on European temperatures.

Acknowledgments. The authors thank T. Woollings (University of Reading, United Kingdom) and participants of the 2016 SPARC workshop on atmospheric blocking (Reading, United Kingdom) for fruitful discussions and helpful comments, and S. Morak (University of Edinburgh, UK) for results from earlier work. We acknowledge the E-OBS data from the EU-FP6 project ENSEMBLES (http://ensembles-eu.metoffice.com) and the data providers in the ECA&D project (http://www.ecad.eu). ECMWF (Reading, United Kingdom) is acknowledged for access to its ERA-Interim dataset. This work was funded by the Austrian Science Fund (FWF) under Research Grant W 1256-G15 (Doctoral Programme Climate Change—Uncertainties, Thresholds and Coping Strategies). G. C. Hegerl was supported by the ERC funded project TITAN (EC-320691), by the Wolfson Foundation and the Royal Society as a Royal Society Wolfson Research Merit Award (WM130060) holder, by the EUCLEIA project funded by the European Union's Seventh Framework Programme (FP7/2007–13) under Grant Agreement 607085, and by NCAS. The authors thank the editor D. Waugh and three anonymous reviewers for their helpful comments on the manuscript.

REFERENCES

AGRI4CAST, 2016: JRC MARS Bulletin—Crop monitoring in Europe. European Commission/Joint Research Centre, 41 pp. [Available online at https://ec.europa.eu/jrc/sites/default/files/jrc-mars-bulletin-vol24-no5.pdf.]

Barriopedro, D., R. García-Herrera, A. R. Lupo, and E. Hernández, 2006: A climatology of Northern Hemisphere blocking. *J. Climate*, **19**, 1042–1063, doi:10.1175/JCLI3678.1.

——, ——, and R. Huth, 2008: Solar modulation of Northern Hemisphere winter blocking. *J. Geophys. Res.*, **113**, D14118, doi:10.1029/2008JD009789.

——, ——, and R. M. Trigo, 2010: Application of blocking diagnosis methods to general circulation models. Part I: A novel detection scheme. *Climate Dyn.*, **35**, 1373–1391, doi:10.1007/s00382-010-0767-5.

Bieli, M., S. Pfahl, and H. Wernli, 2015: A Lagrangian investigation of hot and cold temperature extremes in Europe. *Quart. J. Roy. Meteor. Soc.*, **141**, 98–108, doi:10.1002/qj.2339.

Brunner, L., A. K. Steiner, B. Scherllin-Pirscher, and M. W. Jury, 2016: Exploring atmospheric blocking with GPS radio occultation observations. *Atmos. Chem. Phys.*, **16**, 4593–4604, doi:10.5194/acp-16-4593-2016.

Buehler, T., C. C. Raible, and T. F. Stocker, 2011: The relationship of winter season North Atlantic blocking frequencies to extreme cold or dry spells in the ERA-40. *Tellus*, **63A**, 212–222, doi:10.1111/j.1600-0870.2010.00492.x.

Cassou, C., and J. Cattiaux, 2016: Disruption of the European climate seasonal clock in a warming world. *Nat. Climate Change*, **6**, 589–594, doi:10.1038/nclimate2969.

——, L. Terray, and A. S. Phillips, 2005: Tropical Atlantic influence on European heat waves. *J. Climate*, **18**, 2805–2811, doi:10.1175/JCLI3506.1.

Cattiaux, J., R. Vautard, C. Cassou, P. Yiou, V. Masson-Delmotte, and F. Codron, 2010: Winter 2010 in Europe: A cold extreme in a warming climate. *Geophys. Res. Lett.*, **37**, L20704, doi:10.1029/2010GL044613.

Croci-Maspoli, M., C. Schwierz, and H. C. Davies, 2007: A multifaceted climatology of atmospheric blocking and its recent linear trend. *J. Climate*, **20**, 633–649, doi:10.1175/JCLI4029.1.

Davini, P., C. Cagnazzo, S. Gualdi, and A. Navarra, 2012: Bidimensional diagnostics, variability, and trends of Northern Hemisphere blocking. *J. Climate*, **25**, 6496–6509, doi:10.1175/JCLI-D-12-00032.1.

——, ——, P. G. Fogli, E. Manzini, S. Gualdi, and A. Navarra, 2014: European blocking and Atlantic jet stream variability in the NCEP/NCAR reanalysis and the CMCC-CMS climate model. *Climate Dyn.*, **43**, 71–85, doi:10.1007/s00382-013-1873-y.

Dee, D. P., and Coauthors, 2011: The ERA-Interim reanalysis: Configuration and performance of the data assimilation system. *Quart. J. Roy. Meteor. Soc.*, **137**, 553–597, doi:10.1002/qj.828.

Haylock, M. R., N. Hofstra, A. M. G. Klein Tank, E. J. Klok, P. D. Jones, and M. New, 2008: A European daily high-resolution gridded data set of surface temperature and precipitation for 1950–2006. *J. Geophys. Res.*, **113**, D20119, doi:10.1029/2008JD010201.

Hufkens, K., M. A. Friedl, T. F. Keenan, O. Sonnentag, A. Bailey, J. O'Keefe, and A. D. Richardson, 2012: Ecological impacts of a widespread frost event following early spring leaf-out. *Global Change Biol.*, **18**, 2365–2377, doi:10.1111/j.1365-2486.2012.02712.x.

IPCC, 2013: *Climate Change 2013: The Physical Science Basis*. T. F. Stocker et al., Eds., Cambridge University Press, 1535 pp.

Klok, E. J., and A. M. G. Klein Tank, 2009: Updated and extended European dataset of daily climate observations. *Int. J. Climatol.*, **29**, 1182–1191, doi:10.1002/joc.1779.

Ma, S., A. J. Pitman, R. Lorenz, J. Kala, and J. Srbinovsky, 2016: Earlier green-up and spring warming amplification over Europe. *Geophys. Res. Lett.*, **43**, 2011–2018, doi:10.1002/2016GL068062.

Matsueda, M., 2011: Predictability of Euro-Russian blocking in summer of 2010. *Geophys. Res. Lett.*, **38**, L06801, doi:10.1029/2010GL046557.

Menzel, A., R. Helm, and C. Zang, 2015: Patterns of late spring frost leaf damage and recovery in a European beech (*Fagus sylvatica* L.) stand in south-eastern Germany based on repeated digital photographs. *Front. Plant Sci.*, **6**, 110, doi:10.3389/fpls.2015.00110.

Morak, S., G. C. Hegerl, and N. Christidis, 2013: Detectable changes in the frequency of temperature extremes. *J. Climate*, **26**, 1561–1574, doi:10.1175/JCLI-D-11-00678.1.

Pelly, J. L., and B. J. Hoskins, 2003: A new perspective on blocking. *J. Atmos. Sci.*, **60**, 743–755, doi:10.1175/1520-0469(2003)060<0743:ANPOB>2.0.CO;2.

Pfahl, S., and H. Wernli, 2012: Quantifying the relevance of atmospheric blocking for co-located temperature extremes in the Northern Hemisphere on (sub-)daily time scales. *Geophys. Res. Lett.*, **39**, L12807, doi:10.1029/2012GL052261.

Rex, D. F., 1950: Blocking action in the middle troposphere and its effect upon regional climate I: An aerological study of blocking action. *Tellus*, **2**, 196–211, doi:10.1111/j.2153-3490.1950.tb00331.x.

Scherrer, S. C., M. Croci-Maspoli, C. Schwierz, and C. Appenzeller, 2006: Two-dimensional indices of atmospheric blocking and their statistical relationship with winter climate patterns in the Euro-Atlantic region. *Int. J. Climatol.*, **26**, 233–249, doi:10.1002/joc.1250.

Sillmann, J., M. Croci-Maspoli, M. Kallache, and R. W. Katz, 2011: Extreme cold winter temperatures in Europe under the influence of North Atlantic atmospheric blocking. *J. Climate*, **24**, 5899–5913, doi:10.1175/2011JCLI4075.1.

Stefanon, M., F. D'Andrea, and P. Drobinski, 2012: Heatwave classification over Europe and the Mediterranean region. *Environ. Res. Lett.*, **7**, 014023, doi:10.1088/1748-9326/7/1/014023.

Tibaldi, S., and F. Molteni, 1990: On the operational predictability of blocking. *Tellus*, **42A**, 343–365, doi:10.1034/j.1600-0870.1990.t01-2-00003.x.

Trigo, R. M., I. F. Trigo, C. C. DaCamara, and T. J. Osborn, 2004: Climate impact of the European winter blocking episodes from the NCEP/NCAR reanalyses. *Climate Dyn.*, **23**, 17–28, doi:10.1007/s00382-004-0410-4.

Whan, K., F. Zwiers, and J. Sillmann, 2016: The influence of atmospheric blocking on extreme winter minimum temperatures in North America. *J. Climate*, **29**, 4361–4381, doi:10.1175/JCLI-D-15-0493.1.

Woollings, T., 2010: Dynamical influences on European climate: An uncertain future. *Philos. Trans. Roy. Soc.*, **368A**, 3733–3756, doi:10.1098/rsta.2010.0040.

Xoplaki, E., J. F. González-Rouco, J. Luterbacher, and H. Wanner, 2003: Mediterranean summer air temperature variability and its connection to the large-scale atmospheric circulation and SSTs. *Climate Dyn.*, **20**, 723–739, doi:10.1007/s00382-003-0304-x.

Zwiers, F. W., X. Zhang, and Y. Feng, 2011: Anthropogenic influence on long return period daily temperature extremes at regional scales. *J. Climate*, **24**, 881–892, doi:10.1175/2010JCLI3908.1.